7/20/04 5:25 PM (2556 words)

An Extended AVHRR 8-km NDVI Data Set Compatible with MODIS and SPOT Vegetation NDVI Data

Compton J. Tucker, Jorge E. Pinzon, Molly E. Brown, Daniel A. Slayback, Edwin W. Pak, Robert Mahoney, Eric F. Vermote, and Nazmi El Saleous

Laboratory for Terrestrial Physics
Biospheric Sciences Branch, Code 923
NASA/Goddard Space Flight Center
Greenbelt, Maryland 20771 USA

contact: compton.j.tucker@nasa.gov //01 301 614-6644

Abstract: Daily daytime Advanced Very High Resolution Radiometer 4-km global area coverage data have been processed to produce a normalized difference vegetation index 8-km equal-area data set from July 1981 through December 2003 for all continents except Antarctica. New features of this data set include bimonthly composites, NOAA-9 descending node data from September 1994 to January 1995, volcanic stratospheric aerosol correction for 1982-1984 and 1991-1994, normalized difference vegetation index normalization using empirical mode decomposition/reconstruction to minimize solar zenith angle effects, inclusion of data from NOAA-16 for 2000-2003, and a similar dynamic range with the MODIS normalized difference vegetation index. Data fields available include the normalized difference vegetation index; thermal radiances from channel 4 and channel 5; solar zenith angle, zenith view angle, and view azimuth angle; and the date of each pixel. Post-processing review corrected the majority of dropped scan lines, navigation errors, data drop outs, edge-of-orbit composite discontinuities, and other artifacts in the composite normalized difference vegetation index data. All data are available from the University of Maryland Global Land Cover Facility (http://glcf.umiacs.umd.edu).

Introduction

A consistent and long record of remote sensing data is crucial for trend analysis in climate studies. New improved coarse-resolution global land surface satellite data are available from SeaWiFS (October 1997 – present), SPOT-4's Vegetation Sensor (May 1998 – present), and NASA's moderate resolution imaging spectrometers (MODIS) on the Terra and Aqua platforms (January 2000 – present and December 2002 - present, respectively) (Table 1). Although significant improvements have been made with new, global, land vegetation-sensing instruments, the existing July 1981 to the present 4-km archive of data from the advanced very high resolution radiometer (AVHRR) instrument is an invaluable and irreplaceable archive of historical land surface information. This archive of global 4-km AVHRR data results from five different AVHRR instruments on five different NOAA polar-orbiting meteorological satellites (Cracknell 1997, Kidwell 1999). If the 1981-2003 record of AVHRR data could be processed in a consistent and quantitatively comparable manner with the new generation of sensors mentioned above, the global land surface satellite climate

data record acquires an additional ~19 years to compliment the 5+ years of data presently in hand from the improved sensors listed in Table 1.

Spectral Vegetation Indices

Spectral vegetation indices are usually composed of red and near infrared radiances or reflectances, sometimes with additional channels included (Tucker 1979). They are highly correlated with the photosynthetically-active biomass, chlorophyll abundance, and energy absorption (reviewed in Myneni *et al*. 1995). The use of spectral vegetation indices derived from AVHRR satellite data followed the launch of NOAA-6 in June 1979 and NOAA-7 in July 1981 (Gray and McCrary 1981, Schneider *et al.* 1981, Townshend and Tucker 1981).[1] Since then, the normalized difference vegetation index (NDVI) has become the most used product derived from NOAA AVHRR data (Cracknell 2001), largely from the use of NDVI data sets formed via maximum value compositing (Holben 1986). Composite NDVI data minimize cloud and atmospheric contamination without corrections to the channel 1 and channel 2 radiance data in question. While spectral vegetation indices are the most widely used of any of the products derived from the AVHRR instruments, this was never anticipated by the designers of the AVHRR instruments who had no idea what a vegetation index was. AVHRR NDVI data have been used extensively since 1981 to study global land processes (reviewed in Townshend 1994, D'Souza *et al*. 1996, Cracknell 1997, and Defries and Belward 2000, among others).

An unfortunate feature of the AVHRR is the first two channels span considerable spectral intervals (**figure 1**). This complicates *ex post facto* absolute calibration of these reflective channels and makes atmospheric correction more difficult (Tanre et al. 1992). An alternative to maximum value compositing is to: (1) correct AVHRR channel 1 and 2 data for atmospheric effects such as Raleigh scattering, ozone absorption, aerosols, and water vapor absorption; (2) make a bi-directional reflectance distribution function correction to the atmospherically-corrected channel 1 and 2 data and use this to correct the viewing geometry to a constant viewing perspective; (3) screen for clouds; and (4) form a composite image. This is more easily done for narrow spectral bands, where single effects usually occur within the band in question, rather than the extremely wide spectral bands for AVHRR channel 1 and 2 (figure 1). We have chosen to focus upon the NDVI and not include channel 1 and channel 2 normalized radiances in our new and extended AVHRR NDVI data set. We continue to work on providing calibrated AVHRR channel 1 and channel 2 radiances for the 1981 to 2003 period and will release these data when we have minimized extraneous effects in the channel 1 and channel 2 radiance data.

Previous AVHRR-derived global land surface NDVI data include the NOAA global vegetation index (GVI) (Tarpley *et al.* 1984), the NASA Pathfinder 8-km data set (James and Kalluri 1994), and data set produced by the European Space Agency at the Joint Research Center in Italy (Malingreau and Belward 1994). Tucker *et al.* (1994) and Los *et al.* (1994) described early AVHRR NDVI data sets produced at NASA/Goddard Space Flight Center. AVHRR 1-km land surface data sets were produced for a limited time by Eidenshink and

[1] The AVHRR instruments on NOAA-6 and NOAA-7 s were the first in the TIROS-N series of satellites to have non-overlapping channel 1 and channel 2 spectral bands. Overlapping red and near-infrared spectral bands precludes calculating a NDVI. The NDVI is calculated as NDVI = (channel 2 - channel 1)/(channel 2 + channel 1) (figure 1).

Faundeen (1994) (Table 1). We now describe a new improved normalized difference vegetation index and associated layer data set available to the research community.

Data Processing

Satellite data in NOAA level-1b format (Kidwell 1997) were ingested from magnetic media, were forward mapped to the output bin closest to the center location of each 8 km equal area grid cell, respective calibration values were applied to each channel (Vermote and Kaufman 1995), and the other values associated with the maximum NDVI were retained for each compositing period (Table 1).

We used a similar navigation procedure to El Saleous *et al.* (2000), which in turn is based upon the work of Baldwin and Emery (1995). The orbital model predicts the position of the satellite at any time, using the satellite on-board clock and orbital elements to determine the predicted position. From this perspective, the sun-target-sensor geometry is determined. The NOAA satellites' velocity with respect to the earth's surface is ~7 km/second and the output bin size we employed is 8 km. This translates into a timing error of $< \pm 1.0$ second to achieve a navigation accuracy of $< \pm$ 1 pixel. The majority of our navigation errors were due to errors of the on-board spacecraft clock.

Every composite image was manually checked for navigation accuracy by comparing the mapped data to a reference coastline for the continent in question. Images with > □ 1 pixel navigation error were investigated and the day(s) of the navigation error identified. These days were subsequent reprocessed separately and manually registered to the reference data, to bring the badly navigated day(s) into agreement with the reference coastline, and the composite image was reconstructed by maximum value NDVI compositing. In a few cases it was necessary to discard data from specific days, as the navigation errors were impossible to adjust.

With the failure of NOAA-13 to achieve orbit in 1992, NOAA-11 continued to provide global afternoon/early morning AVHRR data. By 1994, the afternoon equatorial overpass time for NOAA-11 was ~ 17:00 hours. We began using NOAA-9 descending node AVHRR data for our global NDVI data set in September 1994, and continued using these data until NOAA-14 became operational in late January 1995.[2] There is thus a fundamental difference between the PAL and GVI data sets and the data set we describe herein: We use NOAA-9 AVHRR data from October 1994 into January 1995 when there were no NOAA-11 AVHRR data (it had failed), and use NOAA-9 AVHRR data in September 1994 when the PAL and GVI data sets use NOAA-11 data.

Radiometric calibration

Satellite determination of long-term surface trends requires precision within and among various space-borne instruments. It is also crucial to document the within- and among-sensor calibration uncertainty to determine the accuracy with which surface trends over time can be ascertained. The NDVI data we describe were processed in two ways: (1) NOAA-7 through NOAA-14 channel 1 and 2 data from were processed using the Vermote and Kaufman (1995) channel 1 and channel 2 calibration. The resulting NDVI fields were

[2] NOAA-9 had a day time descending node equatorial crossing time of ~09:00 hours in mid-1994 to early 1995. It had "rocked around the clock", with a ~2-3 minute/month later time procession from its original day time descending node equatorial crossing time of 02:30 hours.

further adjusted using the technique of Los (1998), then decomposed and reconstructed using empirical mode decomposition to correct for solar zenith angle effects (Pinzon 2002); and (2) Data from NOAA-16 were processed using the preflight channel 1 and channel 2 calibration values and formed into maximum values composites. An empirical mode decomposition and reconstruction was performed to insure a slope with respect to time of 0.00 in desert areas and was also used to correct solar zenith angle artifacts. This NOAA-16 NDVI time series was adjusted by a constant offset to match up with a coincident-in-time and spatially-aggregated 8-km SPOT Vegetation NDVI time series, which had previously been adjusted to match up with the corresponding coincident-in-time NOAA-14 NDVI time series. We thus used overlapping SPOT Vegetation NDVI time series as the means to intercalibrate or tie together the NOAA-14 and NOAA-16 NDVI time series (Pinzon et al. 2004). This was necessary because the bi-linear gain for channel 1 and channel 2 of NOAA-16's AVHRR instrument complicates *ex post facto* calibration. Thermal calibration coefficients after Weinrab *et al.* (1990) were used for the calibration of all thermal channels.

Atmospheric Correction and Cloud Screening

We choose to produce a maximum value NDVI composite data set, and associated layers, without any atmospheric correction, except during the El Chichon and Mt. Pinatubo volcanic stratospheric aerosol periods. A stratospheric aerosol correction was applied as proposed by Vermote *et al.* (1997) from April 1982 through December 1984 and from June 1991 through December 1994. We formed composite stratospheric aerosol optical depth fields by combining the work of Sato *et al.* (1993), Hansen *et al.* (1997), and Vermote *et al.* (1997). Rosen *et al.* (1994), Russel et al. (1993) and Dutton (1994) were used to compare specific optical depth measurements to our blended global fields. We produced optical depth fields that varied by month and degree of latitude (figure 2).

Cloud screening was provided by a channel 5 thermal mask of 0^{o} C for all continents except Africa, where a cloud mask of 10^{o} C was used. In addition, the bimonthly composites significantly reduced cloud contamination and the channel 4 and channel 5 thermal values are available for *ex post facto* cloud screening if desired.

Solar Zenith Angle Correction

Orbital drift of the "afternoon" NOAA satellites (Cracknell 1997) significantly affects sun-target-sensor geometry and introduces associated NDVI errors which vary with latitude, green leaf density, and vegetation structure (Kaufmann *et al*. 2000). We performed a solar zenith angle correction to the NDVI data using the adaptive empirical mode decomposition method of Pinzon *et al.* (2004). The empirical mode decomposition method accounts for local variation in solar zenith angle and embedded nonlinear and non-stationary variations. We are able to account for ~90% of the solar zenith angle affect upon the NDVI at all latitudes, remove these effects from the NDVI data, and reconstruct the NDVI data without the solar zenith angle variation. Our solar zenith angle corrections were greatest in the tropics for tropical forests, moderate in the tropics for less-densely vegetated areas, and lowest at higher northern and lower southern latitudes (figure 3).

The challenge when making needed corrections to the multi-instrument AVHRR continuum of observations is to correct for calibration variations, solar zenith angle, stratospheric aerosol effects, etc. while not removing variation in the data caused by surface conditions. In our opinion, Cihlar *et al.* (1999) and Gutman (1999) "over corrected" their

AVHRR data sets, and in the process, reduced or demolished natural trends in their data. They then concluded that AVHRR data cannot be used to study inter-annual NDVI variations over the record of NOAA AVHRR NDVI data. We found it was possible to correct the AVHRR NDVI 1981-2003 record for many extraneous effects while retaining natural surface variations in the data.

Assessment NDVI Data Quality

We assessed the quality of our new AVHRR NDVI data set by looking at a variety of targets through time. We first compared our time series NDVI observations with desert targets at different latitudes, desert targets which were not used in the channel 1 and 2 calibration nor the NDVI normalization procedure. We found the NDVI vs. time trends or slopes to be very close to zero, within and among the different satellite periods, for all the deserts studied, without any apparent discontinuities (figure 4).

We also compared our data set to the Pathfinder PAL and GVI data sets. The Pathfinder AVHRR Land NDVI data (James and Kalluri 1994) and GVI data (National Climate Data Center 2003) show considerable more interannual variation than the new GIMMS data (figure 5). In particular, the 1991-1995 time period is suspect for both the PAL and GVI data. We explain these differences as the GIMMS data have been more thoroughly reviewed, have a stratospheric aerosol correction for the 1991-1993 Mt. Pinatubo volcanic period, and use data from NOAA-9 in late 1994 rather than data from NOAA-11. In addition, the PAL and GVI data have no data from October 1994 to late January 1995, as NOAA-11's AVHRR instrument had failed during this time. In contrast, the AVHRR NDVI data described herein used descending node ~09:00 equatorial crossing time data from NOAA-9 from September 1994 until late January 1995.

MODIS and SPOT Vegetation data from the present Terra and Aqua platforms represents a tremendous improvement in the ability to monitor land photosynthetic capacity. We have been able to process the AVHRR NDVI 1981 to 2003 historical record within the MODIS NDVI data dynamic range (figure 6). This enables the many advantages of MODIS and SPOT Vegetation data to be used while retaining historical information from areas of interest, albeit at a much reduced spatial resolution. The data we describe can be obtained the Global Land Cover Facility at the University of Maryland (glcf.umiacs.umd.edu). Papers using the data we describe herein have reported stability of these data for studying 1981 to 2003 interannual variation of global drought phenomena (Lotsch et al. 2003), the effect of the 1991 Mt. Pinatubo volcanic eruption upon global net primary production (Angert et al. 2004a), the interaction of higher-latitude warming and drier summers (Angert et al. 2004b), atmospheric circulation changes and continental drought (Buermann et al. 2004), interannual variability of the NDVI from Amazonia (Poveda and Salazar 2004), and the greening of arctic Alaska (Jia et al. 2003). All data are available from the University of Maryland Global Land Cover Facility (http://glcf.umiacs.umd.edu).

Acknowledgements: The data set we describe would not have been possible without the work of two people: Martha Maiden and Stanley Schneider. We thank Martha Maiden of NASA Headquarters for her support that made this data set possible. We thank Stanley Schnieder for convincing NOAA management in 1977 to alter the spectral configuration of the TIROS-N channel one band pass from 0.55-0.90 μm to 0.55-0.70 μm. None of the extensive and widespread AVHRR NDVI work would be possible without Schneider's

unilateral action in 1977 which restricted AVHRR channel 1 to the upper portion (0.55-0.70 μm) of the visible spectrum.

References

ANGERT, A., BIRAUD, S., BONFILS, C., BUERMANN, W., and FUNG, I. Y., 2004a, CO_2 seasonality indicates origins of post-Pinatubo sink, *Geophysical Research Letters,* **31**, 1103-1107.

ANGERT, A., TUCKER, C. J., BIRAUD, S., BONFILS, C., HENNING, C., BUERMANN, W., and FUNG, I. Y., 2004b, Drier summers cancel out the CO2 uptake enhancement induced by warmer winters, *Nature* (submitted).

BUERMANN, W., LINTNER, B., ANGERT, A., KOVEN, C. D., TUCKER, C. J., and FUNG, I. Y., 2004, Identification of circulation changes and continental drought in the Mauna Loa CO2 record, *Science* (submitted).

BALDWIN, D. and EMERY, W. J., 1995, Spacecraft attitude variations of NOAA-11 inferred from AVHRR imagery, *International Journal of Remote Sensing*, **16**, 531-548.

CIHLAR, J., CHEN, J. M., LI, Z., HUANG, F., LATIFOVIC, R., and DIXON, R., 1998, Can interannual land surface signal be discerned in composite AVHRR data?, *Journal of Geophysical Research,* **103**, 23163-23172.

CRACKNELL, A. P., 1997, *The Advanced Very High Resolution Radiometer*, Taylor and Francis, London, 534 p.

CRACKNELL, A. P., 2001, The exciting and totally unanticipated success of the AVHRR in applications for which it was never intended, *Advances in Space Research* **28**, 233-240.

DEFRIES, R. S. and BELWARD, A. S., 2000, Global and regional land cover characterization from satellite data, *International Journal of Remote Sensing*, **21**, 1083-1092.

DUTTON E., GREDDY, P., RYAN, S., and DELUISI, J. J., 1994, Features and effects of aerosol optical depth observed at Mauna-Loa, Hawaii - 1982-1992, *Journal of Geophysical Research-Atmospheres,* **99**, 8295-8306.

D'SOUZA, G., BELWARD, A.S., and MALINGREAU, J.P., 1996*, Advances in the Use of NOAA AVHRR Data for Land Applications*, Kluwer Academic Publishers, Dordrecht, Netherlands, 479 p.

EIDENSHINK, J. C. and FAUDEEN, J.L., 1994, The 1 km resolution global data set: needs of the International Geosphere Biosphere Program, *International Journal of Remote Sensing*, **16**, 531-54815:3443-3462.

SALEOUS, N. Z., VERMOTE, E. F., JUSTICE, C. O., TOWNSHEND, J. R. G., TUCKER, C. J., and GOWARD, S. N., 2000, Improvements in the global biospheric record from the advanced very high resolution radiometer, *International Journal of Remote Sensing*, **21**, 1251-1278.

GRAY, T. I. and MCCRARY, D. G., 1981, *Meteorological Satellite Data--A Tool to Describe the Health of the World's Agriculture*, AgRISTARS Report EW-NI-04042, Johnson Space Center, Houston, Texas, 7 p.

GUTMAN, G. G., 1999, On the use of long-term global data of land reflectances and vegetation indices derived from the advanced very high resolution radiometer, *Journal of Geophysical Research,* **104**, 6241-6255.

HANSEN, J., RUEDY, J., SATO, M., and REYNOLDS, R., 1996, Global surface air temperature in 1995: Return to pre-Pinatubo level, *Geophysical Research Letters,* **23**, 1665-1668.

HOLBEN, B.N., 1986, Characteristics of maximum-value composite images from temporal AVHRR data, *International Journal of Remote Sensing*, **7**, 1417-1434.

HOOKER, S. B., ESAIAS, W. E., FELDMAN, G.C., GREGG, W.W., and McCLAIN, C. R., 1992, *An overview of SeaWiFS and Ocean Color*, NASA Tech. Memo. 104566, vol. 1, 24p.

JAMES, M. E. and KALLURI, S. N., 1994, The Pathfinder AVHRR land data set: An improved coarse-resolution data set for terrestrial monitoring, *International Journal of Remote Sensing*, **15**, 3347-3363.

JIA, G. J., EPSTEIN, H. E., and WALKER, D. A., 2003, Greening of arctic Alaska, 1981-2001, *Geophyscial Research Letters*, 30, 1029-1033.

JUSTICE, C. O., VERMOTE, E., TOWNSHEND, J. R. G., DEFRIES, R., ROY, D. P., HALL, D. K., SALOMONSON, V. V., PRIVETTE, J. L., RIGGS, G., STRAHLER, A., LUCHT, W., MYNENI, R. B., KNYAZIKHIN, Y., RUNNING, S. W., NEMANI, R. R., WAN, Z. M., HUETE, A. R., VAN LEEUWEN, W., WOLFE, R. E., GIGLIO, L., MULLER, J. P., LEWIS, P., and BARNSLEY, M. J., 1998, The Moderate Resolution Imaging Spectroradiometer (MODIS): Land remote sensing for global change research, *IEEE Transactions on Geoscience and Remote Sensing,* 36, 1228-1249.

JUSTICE, C. O. and TOWNSHEND, J. R. G., 1994, Data sets for global remote sensing: lessons learnt, *International Journal of Remote Sensing*, **15**, 3621-3639.

KAUFMANN, R.K., ZHOU, L., KNYAZIKHIN, Y., SHABANOV, N., MYNENI, R., and TUCKER, C.J., 2000, Effect of orbital drift and sensor changes on the time series of AVHRR vegetation index data, *IEEE Transactions on Geoscience and Remote Sensing,* **38**, 2584-2597.

KIDWELL, K. B., 1997, *Polar Orbiter Data Users' Guide (TIROS-n, NOAA-6, NOAA-7, NOAA-8, NOAA-9, NOAA-10, NOAA-11, NOAA-12, and NOAA-14)*, National Oceanic and Atmospheric Administration, Washington, D. C.

LOS, S. O., JUSTICE, C. O., and C. J. TUCKER, 1994, A global 1^o x1^o NDVI data set for climate studies derived from the GIMMS continental NDVI data, *International Journal of Remote Sensing*, **15**,3493-3618.

LOS, S. N., 1998, Estimation of the ratio of sensor degradation between NOAA AVHRR channels 1 and 2 from monthly NDVI composites, *IEEE Transactions on Geoscience and Remote Sensing,* **36**, 206-213.

LOTSCH, A., FRIEDL, M. A., ANDERSON, B. T., and TUCKER, C.J., 2003, Coupled vegetation-precipitation variability observed from satellite and climate records, *Geophysical Research Letters,* **30**, 125-132.

MALINGREAU, J. P. and BELWARD, A. S., 1994, Recent activities in the European Community for the creation and analysis of global AVHRR data sets, *International Journal of Remote Sensing*, **15**, 3397-3416.

MYNENI, R. B., HALL, F. G., SELLERS, P. J., and MARSHAK, A. L., 1995, The interpretation of spectral vegetation indexes, *IEEE Transactions on Geoscience and Remote Sensing,* **33**, 481-486.

NATIONAL CLIMATE DATA CENTER, 2003*, NOAA Global Vegetation Index Guide*, NOAA National Climatic Data Center, Ashville, North Carolina USA, 47 p.

PINZON, J. E., BROWN, M. E., and TUCKER, C. J., 2004, Satellite time series correction of orbital drift artifacts using empirical mode decomposition, To appear in *EMD and its Applications*, edited by N. E. Huang and Shen, S. S. P., World Scientific Publishers, Singapore.

POVEDA, G. and L.F. SALAZAR, 2004, Annual and interannual (ENSO) variability of spatial scaling properties of a vegetation index (NDVI) in Amazonia, *Remote Sensing of Environment (in press)*.

ROSBOROUGH, G. W., BALDWIN, D. G., and W. J. EMERY, 1994, Precise AVHRR navigation, *IEEE Transactions on Geoscience and Remote Sensing,* **32**, 644-657.

ROSEN, J., KJOME, N. T., MCKENZIE, R. L., and LILEY, J. B., 1994, Decay of Mount Pinatubo aerosol at midlatitudes in the northern and southern hemispheres, *Journal of Geophysical Research,* **99**, 25733-25739.

RUSSEL, P. B., LIVINGSTON, J. M., DURRON, E. G., PUESCHEL, R. F., REAGAN, J. A., DEFOOR, T. E., BOX, M. A., ALLEN, D., PILEWSKIE, P., HERMAN, B. M., KINNE,

S. A., and HOFMANN, D. J., 1993, Pinatubo and pre-Pinatubo optical-depth spectra: Mauna Loa measurements, comparisons, inferred particle size distributions, radiative effects, and relationships to lidar data, *Journal of Geophysical Research,* 98, 22969-22985.

SAINT, G. 1995, Spot-4 vegetation system--association with high-resolution data for multiscale studies, *Advances in Space Research*, 17, 107-110.

SATO, M., HANSEN, J., MCCORMICK, M. P., and POLLACK, J. B., 1993, Stratospheric aerosol optical depths, 1850-1990, *Journal of Geophysical Research,* **98**, 22987-22994.

SCHNEIDER, S. R., MCGINNIS, D. F., and GATLIN, J. A., 1981, *Use of NOAA AVHRR Visible and Near-Infrared Data for Land Remote Sensing*. NOAA Technical Report NESS 84, NOAA National Earth Satellite Service, Washington, D.C., 48 p

TANRE, D., HOLBEN, B. N., and KAUFMAN, Y. J., 1992, Atmospheric correction algorithm for NOAA-AVHRR products: theory and applications, *IEEE Transactions on Geoscience and Remote Sensing,* **30**, 2231-2248.

TARPLEY, J. P., SCHNEIDER, S. R., and MONEY, R. L., 1984, Global vegetation indices from NOAA-7 meteorological satellite, *Journal of Climate and Applied Meteorology,* **23**, 491-494.

TOWNSHEND, J. R. G., 1994, Global data sets for land applications from the advanced very high resolution radiometer: an introduction, *International Journal of Remote Sensing*, **15**, 3319-3332.

TOWNSHEND, J. R. G. and TUCKER, C. J., 1981, Utility of AVHRR NOAA-6 and -7 for vegetation mapping, In, *Matching Remote Sensing Technologies and Their Applications Proceedings*, Remote Sensing Soceity, London, pp 97-109.

TUCKER, C. J., 1979, Red and photographic infrared linear combinations for monitoring vegetation, *Remote Sensing of Environment,* 8, 127-150.

TUCKER, C. J., NEWCOMB, W. W., and H. E. DREGNE, 1994, Improved data sets for determination of desert spatial extent, *International Journal of Remote Sensing*, 15, 3519-3545.

VERMOTE, E. F. and Y. J. KAUFMAN, 1995, Absolute calibration of AVHRR visible and near-infrared channels using ocean and cloud views, *International Journal of Remote Sensing*, **16**, 2317-2340.

VERMOTE, E., SALEOUS, N. E., KAUFMAN, Y. J., and DUTTON, E., 1997, Data preprocessing: Stratopsheric aerosol perturbing effect on the remote sensing of vegetation: correction method for the composite NDVI after the Pinatubo eruption, *Remote Sensing Reviews*, **15**, 7-21.

WEINREB, M. P., HAMILTON, G. BROWN, S. and KOCZOR , R. J., 1990, Nonlinearity corrections in calibration of Advanced Very High Resolution Radiometer infrared channels, *Journal of Geophysical Research,* **95**, 7381-7388.

Tables and Figures

Table 1. Global coarse-resolution satellite spectral vegetation index data sets.

Instrument	Dates of Coverage	Spatial Resolution (nadir)	Spectral Bands	Global Data Volume (gb/day)	References, comments
NOAA AVHRR					Cracknell 1997; Kidwell 1997.
NOAA-7	07/1981-02/1985	4-km	5	0.6	
NOAA-9	02/1985-09/1988	4-km	5	0.6	
NOAA-11	09/1988-9/1994	4-km	5	0.6	no data after September 1994
NOAA-9-d	9/1994-01/1995	4-km	5	0.6	descending node ~09:00 data
NOAA-14	01/1995-11/2000	4-km	5	0.6	
NOAA-16	11/2000-present	4-km	5	0.6	
SeaWiFS	9/1997-present	4-km	8	0.4	Hooker et al., 1992
SPOT-4 Vegetation	05/1998-present	1-km	4	5	Saint, 1995.
MODIS	01/2000-present	250-1000 m	32	70	Justice et al., 1998.

Table 2. Data layers and associated information for the 1981 to 2003 NDVI data set.

field	Data Layer	Units	Range of Values	Quantization	To Obtain Value
1	NDVI*-sza	ndvi	-1 to +1	16 bit signed	divide by 10000
2	NDVI*	ndvi	-1 to +1	16 bit signed	divide by 1000
3	NDVI	ndvi	-1 to +1	16 bit signed	divide by 1000
4	channel 4 brightness Temperature	brightness T (K)	160-340 K	16 bit signed	divide by 1000
5	channel 5 brightness Temperature	brightness T (K)	160-340 K	16 bit signed	divide by 1000
6	Day of year	day	1-366	16 bit signed	divide by 100
7	Scan zenith angle	degrees	-100 <-> +100	16 bit signed	divide by 100
8	Solar zenith angle	degrees	0 <-> 90	16 bit signed	divide by 100
9	Relative azmuth angle	degrees	-180 <-> +180	16 bit signed	divide by 100

NDVI*: secondary ndvi calibration applied after Pinzon et al., 2004
NDVI*-sza: = 2ndary ndvi calibration + solar zenith angle correction after Pinzon et al., 2003
NDVI: NDVI from Vermote and Kaufman (1995) channel 1 and 2 calibration
Scan zenith angle: negative value = forward scatter; positive value = backscatter

Figure 1. Spectral acceptance of the Advanced Very High Resolution Radiometer instruments in comparison to SPOT Vegetation, SeaWIFS, and the Moderate Resolution Imaging Spectrometer visible and near infrared bands. See also Table 1.

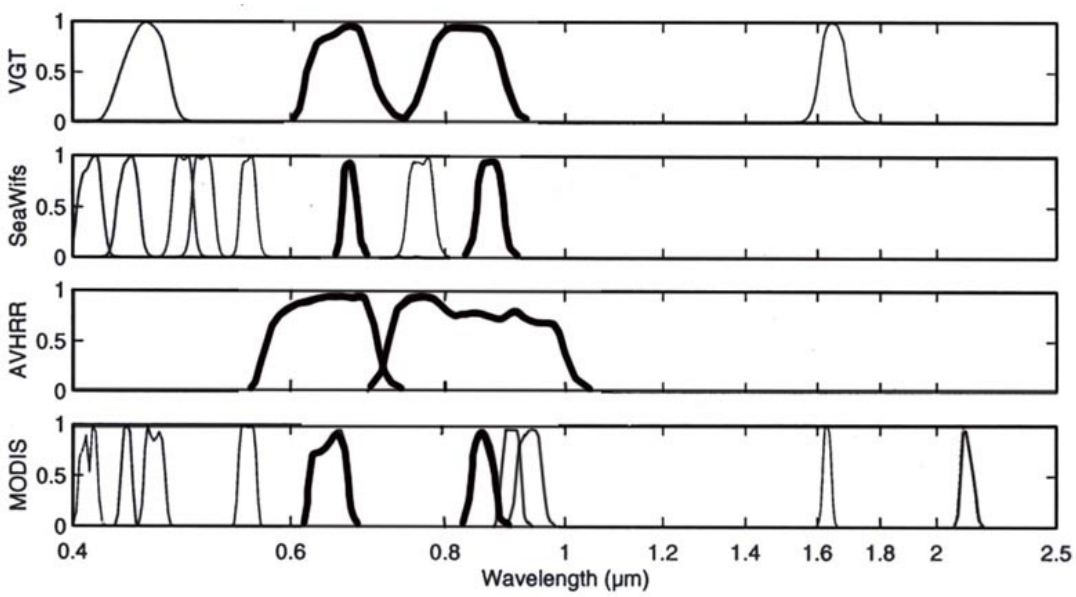

Figure 2. Stratospheric aerosol optical depth from 1982 to 1984 and 1991 to 1993. These two aerosol events were caused by the volcanic eruptions of El Chichon in 1982 and Mt. Pinatubo in 1991. These data were used to correct AVHRR channel 1 and channel 2 data for the 1982-1984 and 1991-1993 periods, respectively.

A.

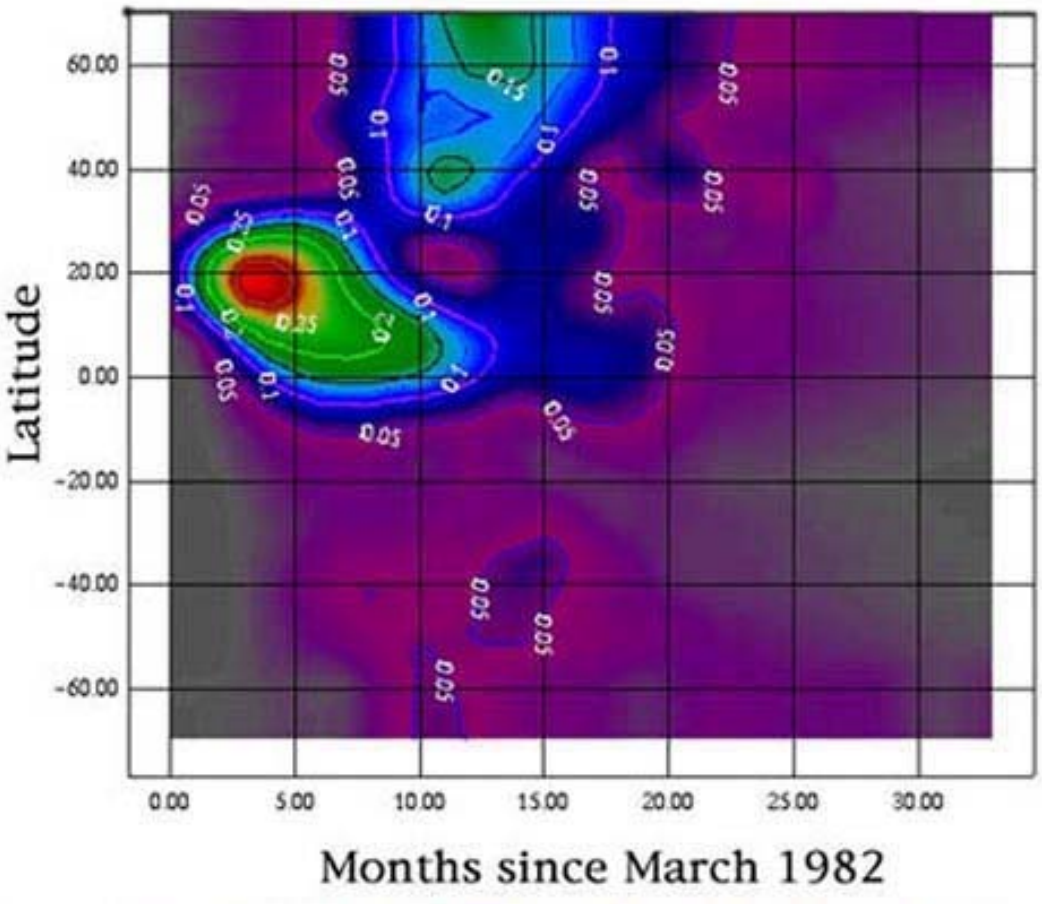

Figure 2B.

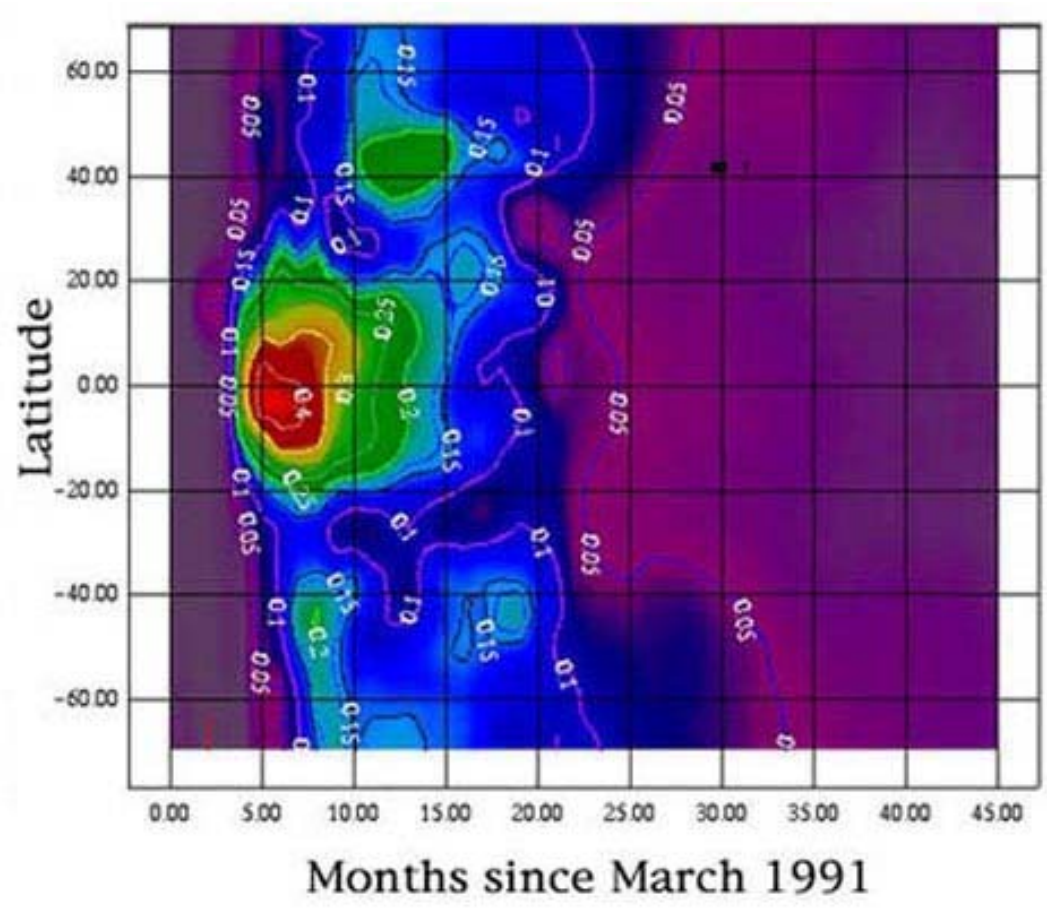
Latitude
60.00
40.00
20.00
0.00
-20.00
-40.00
-60.00
0.00
5.00
10.00
15.00
20.00
25.00
30.00
35.00
40.00
45.00
Months since March 1991

Figure 3. Solar zenith angles vs. time for (A) NOAA-6 (0730 and 1930 hours local solar overpass times) and the series of "afternoon" NOAA satellites from 1981 to 2003 for 1.4 ^{o} N and 18 ^{o} E and (B) NOAA-7 to NOAA-16 for 52.7^{o} N and 106.7^{o} E. Note the procession to later overpass times in each of the afternoon satellite periods (Cracknell 1997). The very late times of NOAA-11 and NOAA-14 are comparable to the overpass time of NOAA-6 at 0730 hours close to the equator. Note the greater annual range in solar zenith angle closer to the equator. This is why solar zenith angle corrections are more important tropically than extra-tropically.

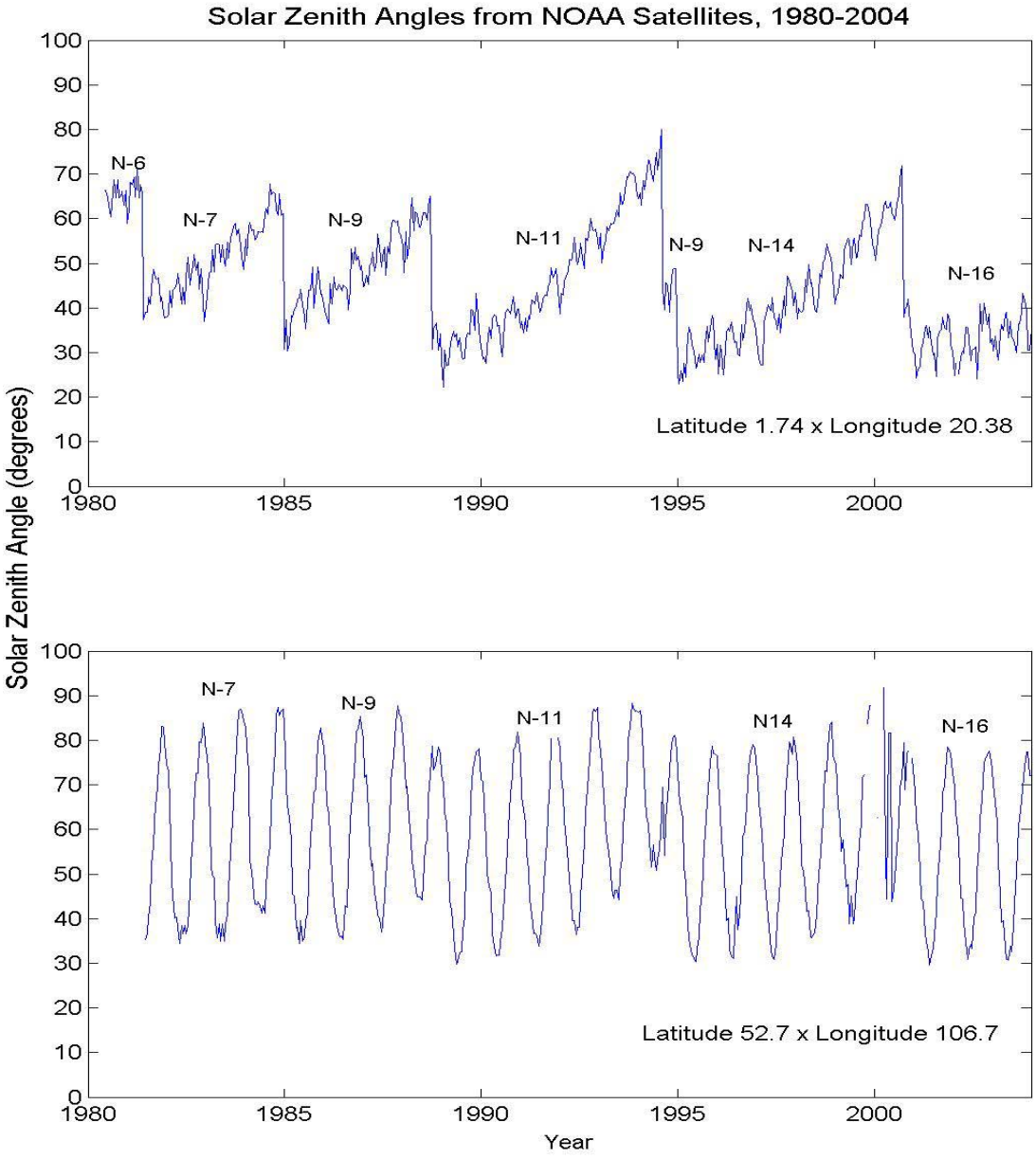

Figure 4. Time series NDVI data from the Arabian Desert (25 ^{o} N, 40 ^{o} E) and Taklamakan Desert (40 ^{o} N, 85 ^{o} E). Note the NDVI vs. time slopes for the Arabian and Taklamakan Deserts are very close to 0.00. Data from the 45 ^{o} to 75 ^{o} N global belt are plotted for comparison. NOTE: this figure is being extended through Dec. 2003.

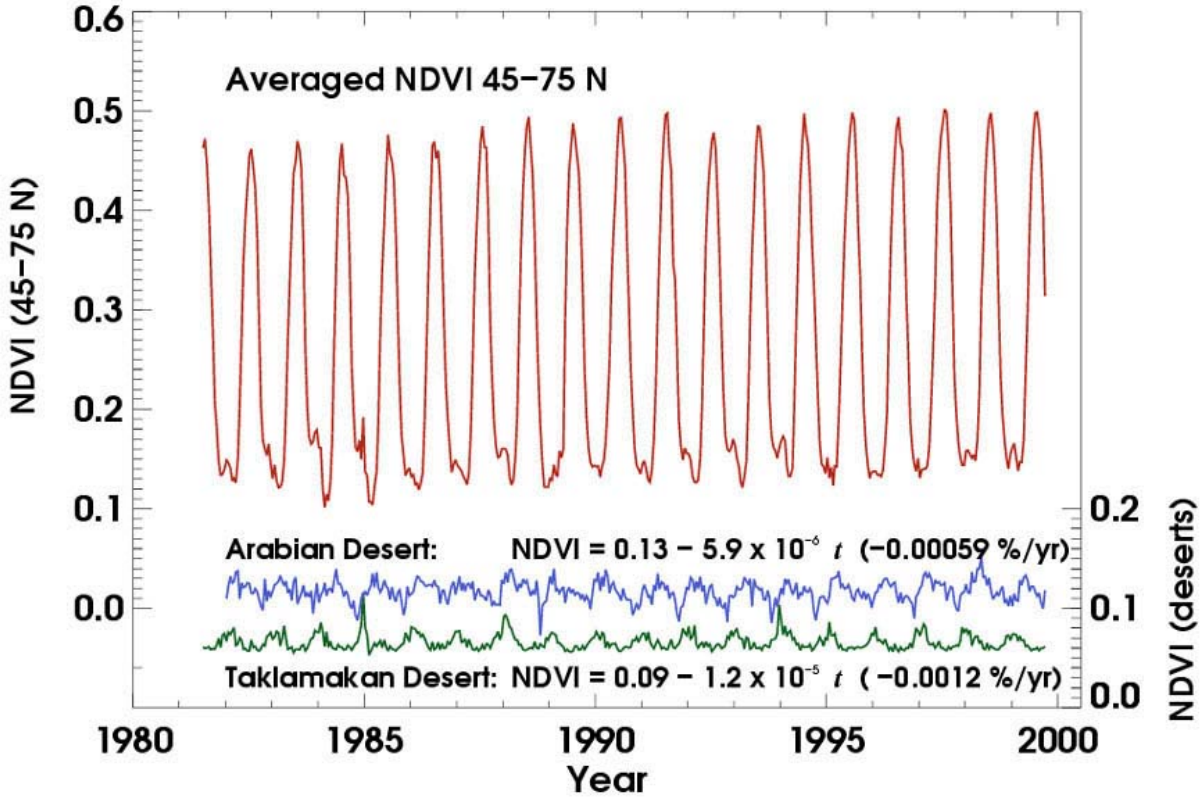

Figure 5. Time series of average annual NDVI by latitude zones for the 1981 to 2000 time period. The PAL NDVI curves were produced from the Pathfinder AVHRR land data set (PAL) distributed by the GSFC Distributed Active Archive Center (James and Kalluri 1994). The GVI curves were produced from the NOAA Global Vegetation Index (National Climate Data Center 2003). The other NDVI curves are derived from the GIMMS data we describe herein, one uncorrected for solar zenith angle effects, and the other corrected for solar zenith angle effects. Note the greater variations among these data sets closer to the equator than towards the poles. See figure 3 for solar zenith angle variations and 4 for NDVI desert stability of the new AVHRR global NDVI data we describe herein.

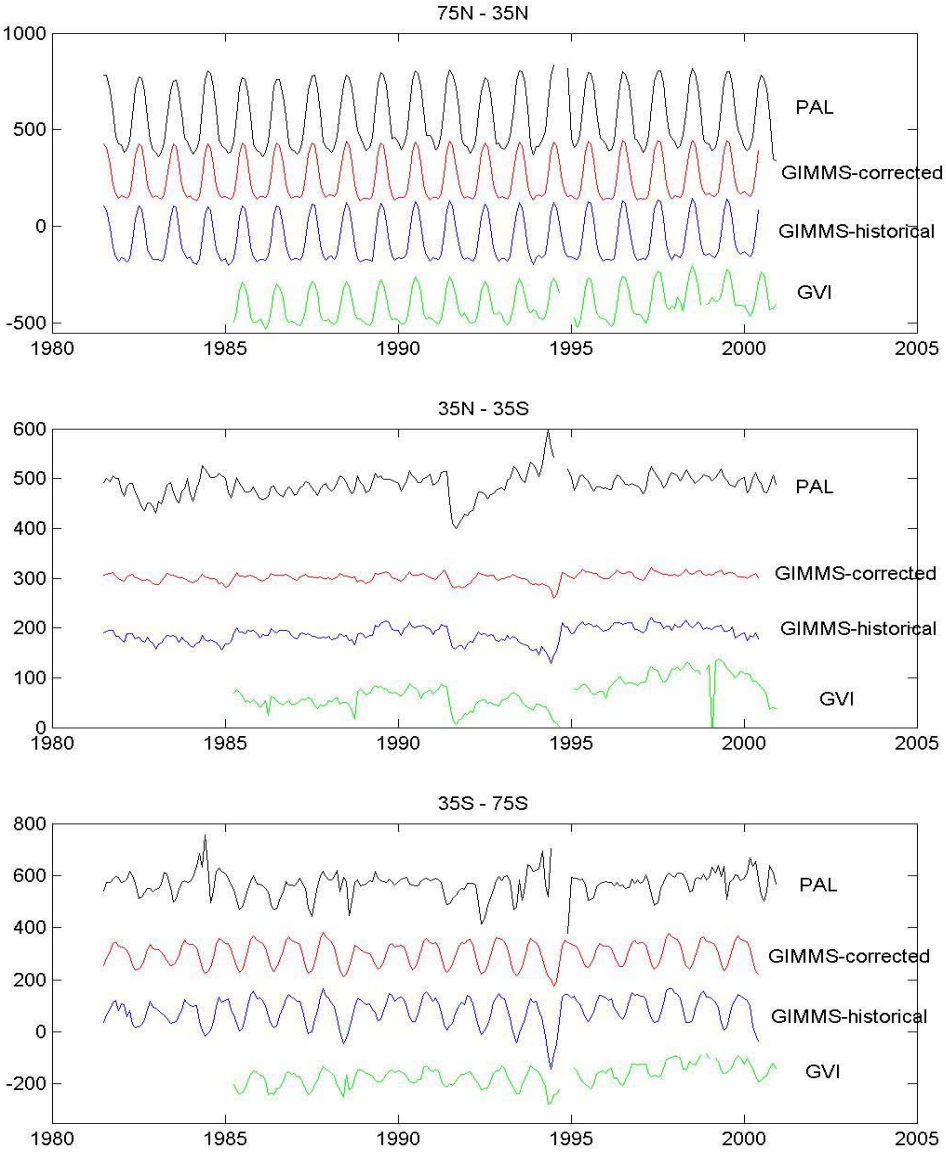

Figure 6. Bondville, Illinois time series plot with the normalized difference vegetation index from four sensors. The AVHRR data we describe in this paper (solid blue line), the Moderate Resolution Imaging Spectrometer (magenta), SPOT-Vegetation (green dashed line), and Landsat-7's Enhanced Thematic Mapper (+ for average and triangles show variations in the scene).